

Connecting blazars with ultra high energy cosmic rays and astrophysical neutrinos

E. Resconi^{1*}, S. Coenders¹, P. Padovani^{2,3}, P. Giommi^{4,5}, L. Caccianiga⁶

¹Technische Universität München, Physik-Department, James-Frank-Str. 1, D-85748 Garching bei München, Germany

²European Southern Observatory, Karl-Schwarzschild-Str. 2, D-85748 Garching bei München, Germany

³Associated to INAF - Osservatorio Astronomico di Roma, via Frascati 33, I-00040 Monteporzio Catone, Italy

⁴Italian Space Agency, ASI, via del Politecnico s.n.c., I-00133 Roma Italy

⁵ICRANet-Rio, CBPF, Rua Dr. Xavier Sigaud 150, 22290-180 Rio de Janeiro, Brazil

⁶INFN sezione di Milano, Dipartimento di Fisica, Università degli Studi di Milano via Celoria 16, 20133 Milano, Italy

19 August 2021

ABSTRACT

We present a strong hint of a connection between high energy γ -ray emitting blazars, very high energy neutrinos, and ultra high energy cosmic rays. We first identify potential hadronic sources by filtering γ -ray emitters in spatial coincidence with the high energy neutrinos detected by IceCube. The neutrino filtered γ -ray emitters are then correlated with the ultra high energy cosmic rays from the Pierre Auger Observatory and the Telescope Array by scanning in γ -ray flux (F_γ) and angular separation (θ) between sources and cosmic rays. A maximal excess of 80 cosmic rays (42.5 expected) is found at $\theta \leq 10^\circ$ from the neutrino filtered γ -ray emitters selected from the second hard *Fermi*-LAT catalogue (2FHL) and for $F_\gamma (> 50 \text{ GeV}) \geq 1.8 \times 10^{-11} \text{ ph cm}^{-2} \text{ s}^{-1}$. The probability for this to happen is 2.4×10^{-5} , which translates to $\sim 2.4 \times 10^{-3}$ after compensation for all the considered trials. No excess of cosmic rays is instead observed for the complement sample of γ -ray emitters (i.e. *not* in spatial connection with IceCube neutrinos). A likelihood ratio test comparing the connection between the neutrino filtered and the complement source samples with the cosmic rays favours a connection between neutrino filtered emitters and cosmic rays with a probability of $\sim 1.8 \times 10^{-3}$ (2.9σ) after compensation for all the considered trials. The neutrino filtered γ -ray sources that make up the cosmic rays excess are blazars of the high synchrotron peak type. More statistics is needed to further investigate these sources as candidate cosmic ray and neutrino emitters.

Key words: neutrinos — radiation mechanisms: non-thermal — BL Lacertae objects: general — gamma-rays: galaxies — pulsars: general — cosmic rays

1 INTRODUCTION

Blazars are Active Galactic Nuclei (AGN) hosting a jet oriented at a small angle with respect to the line of sight with highly relativistic particles moving in a magnetic field and emitting non-thermal radiation (Urry & Padovani 1995). They are among the most luminous and most energetic sources in the Universe. The spectral energy distributions (SEDs) of blazars are composed of two broad humps, a low energy and a high energy one. Blazars are subdivided in two main sub-classes, namely flat-spectrum radio quasars (FSRQ) and BL Lacertae objects (BL Lacs), with the former displaying strong, broad emission lines and the latter instead being characterized by optical spectra showing at

most weak emission lines, sometimes exhibiting absorption features, and in many cases being completely featureless. Based on the rest-frame value of the frequency of the peak of the low energy hump (synchrotron peak, ν_S) blazars of the BL Lac type are called high energy peaked (HBLs) when $\nu_S > 10^{15} \text{ Hz}$ ($> 4 \text{ eV}$). HBLs are the rarest types of blazars, making up $\approx 10\%$ of BL Lacs (Padovani & Giommi 1995), being at the same time very powerful γ -ray emitters. The idea that blazars of various types could be sources of ultrahigh energy cosmic rays (CRs) and, related to that, of high energy neutrinos, has been discussed in e.g. Mannheim (1995); Halzen & Zas (1997) and has since then been explored in a number of studies (see e.g. Muecke et al. 2003; Kistler et al. 2014; Murase et al. 2014; Tavecchio & Ghisellini 2015; Padovani et al. 2015; Kistler & Laha 2016). We perform here detailed statistical studies to test a blazar con-

* E-mail: elisa.resconi@tum.de

nection with CRs going through high energy neutrinos used as “intermediaries” (see [Gaisser et al. 2016](#) for an extensive review of how CRs are accelerated up to $10^{19} - 10^{20}$ eV).

The Pierre Auger Observatory ([Abraham et al. 2004](#); [Aab et al. 2015b](#)) and the Telescope Array (TA) ([Abu-Zayyad et al. 2013b](#)) have collected together more than 300 CRs with $E \geq 52 \times 10^{18}$ eV over the entire sky. The former has detected 231 such events covering mostly the southern hemisphere and the latter 72 events above 57×10^{18} eV covering mostly the northern sky. Despite a series of studies on the CR arrival direction distributions ([Aab et al. 2015a](#); [Abu-Zayyad et al. 2013a](#)), no counterparts have yet been determined. The strongest deviations from isotropy (post-trial probabilities $\sim 1.3 - 1.4\%$) have been obtained for $E \geq 58 \times 10^{18}$ eV in connection with Swift AGN closer than 130 Mpc and more luminous than 10^{44} erg s $^{-1}$, and around the direction of Cen A (at angular separations $\sim 18^\circ$ and $\sim 15^\circ$ respectively) ([Aab et al. 2015a](#)). The distribution of CRs does not present statistically significant small scale structures. However, two “hot” regions ($2 - 3\sigma$ deviations) of about 20° in the CR sky have been reported (see Fig. 1 top, [Abbasi et al. 2014](#), and [Aab et al. 2015a](#)) but their interpretation is not yet clear.

The IceCube South Pole Neutrino Observatory has recently discovered high energy astrophysical neutrinos and has reported a sample of 54 events collected over a period of four years with a deposited energy up to 2 PeV ([Aartsen et al. 2013, 2014](#); [Aartsen et al. 2015a](#)). These events are coming from the entire sky and make up what we define as the Isotropic Neutrino Emission (IvE). They consist of neutrinos of all flavors, which interact inside the instrumented volume (starting events), the majority of which are shower-like¹. The complementary sample of through-going charged current ν_μ from the northern sky has also been studied over a period of six years and recently been reported in [Aartsen et al. \(2016a\)](#) showing that their spectrum is inconsistent with the hypothesis of purely terrestrial origin at the 5.6σ level. The track-like events confirm the general picture of the IvE although their energy spectrum $E^{-\gamma}$ is harder ($\gamma = 2.13 \pm 0.13$) with respect to the all sky one obtained from the starting event sample ($\gamma = 2.58 \pm 0.25$), suggesting a mixed origin of the signal observed by IceCube. Many diverse hypothesis for the astrophysical counterparts of the IvE have been put forward (see, e.g. [Khiali & de Gouveia Dal Pino 2016](#); [Moharana et al. 2016](#); [Murase et al. 2016](#); [Tamborra & Ando 2016](#); [Senno et al. 2016](#); [Wang & Liu 2016](#); [Zirakashvili & Ptuskin 2016](#); [Neronov & Semikoz 2016](#)) but none has so far been statistically supported by the observational data.

In [Padovani et al. \(2016\)](#) the authors have correlated the second catalogue of hard *Fermi*-LAT sources (2FHL) ($E > 50$ GeV, 360 sources of various types, mainly blazars, [Ackermann et al. 2016](#)), and two other catalogs (see Appendix), with the publicly available high energy neutrino sample detected by IceCube ([Aartsen et al. 2014](#); [Aartsen](#)

¹ Shower-like events are one of the topologies for neutrino observatories. Showers have a good energy resolution but reduced angular resolution ($\sim 10^\circ$). The other topology are track-like events induced by muons, that have much better angular resolution ($< 1^\circ$), in which not all the energy is deposited on the detector.

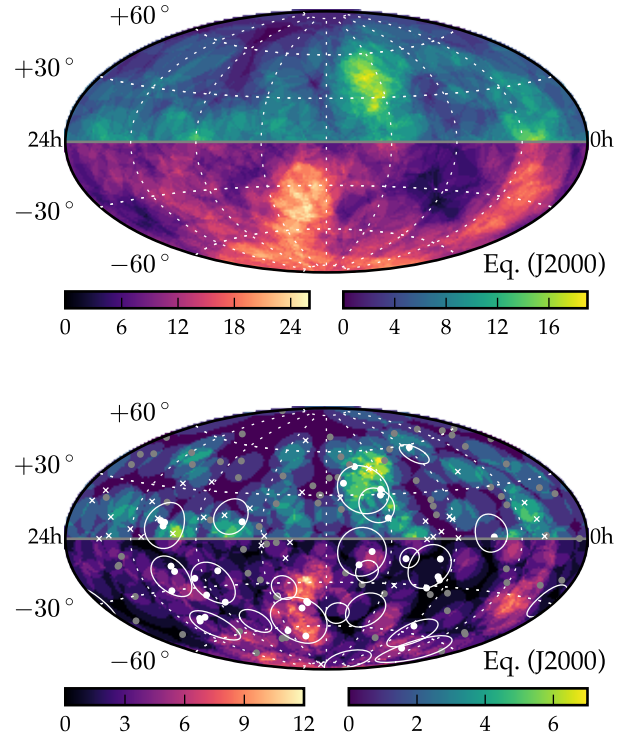


Figure 1. Sky maps in equatorial coordinates: (top) Auger and TA data with uncertainty areas of 20° as reported by the collaborations (and roughly the size of the two hot spots). The color scale indicates the number of events overlapping within the 20° areas; (bottom) Auger and TA data with uncertainty areas of 10° as obtained from our test with overlaid neutrinos contributing to the test (crosses are track-like events, circles are shower-like events with associated median angular error). Dots indicate the 2FHL (HBL + unclassified sample) objects that are filtered (white) or not filtered (grey) by neutrinos as described in the text.

[et al. 2015a](#); [Aartsen et al. 2015b](#); [Schoenen & Raedel 2015](#), including only events with energy and median angular error ≥ 60 TeV and $\leq 20^\circ$ respectively). The probability scanning over F_γ (> 50 GeV) was 0.4%. We have now also evaluated the impact of the trials, which results in a global p-value of 1.4% (2.2σ). This applies only to HBL blazars and appears to be strongly dependent on γ -ray flux.

In [Aartsen et al. \(2016b\)](#), the three collaborations IceCube, Auger, and TA jointly reported about correlation tests between very high energy neutrinos and the same sample of CRs used in this paper. All the studies were compatible with the null hypothesis of no correlation although two interesting excesses were observed when considering IceCube shower-like events: a post-trial probability of 0.05% for an angular scale of 22° provided by the comparison to a randomized CR sky, and a probability of 0.85% obtained by scrambling the neutrinos, thus preserving the existing anisotropies observed in the arrival directions of the CRs. As also discussed in [Aartsen et al. \(2016b\)](#), the first result (CR randomization), is affected by the presence of anisotropies (hot spots) in the CR sky (see Fig. 1, bottom). More interesting is the second result (neutrino randomization), which

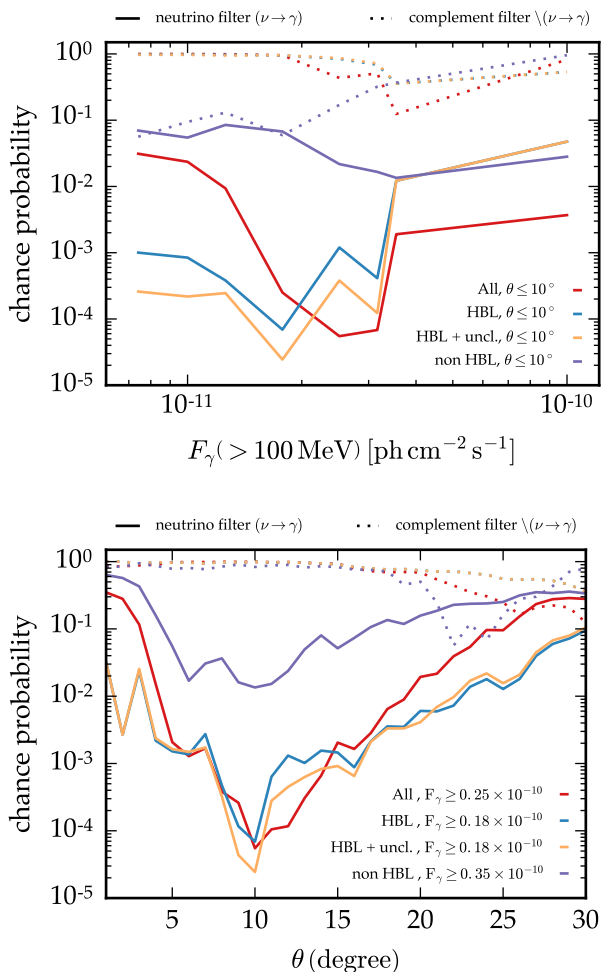


Figure 2. ($\nu \rightarrow \gamma \rightarrow \text{CR}$) correlation test results (2FHL): (top) F_γ projection of the chance probability at a fixed angular distance θ . (bottom) θ projection of the chance probability at a fixed F_γ value. The probabilities are reported for the neutrino filtered γ -ray emitters (solid line) and for the complement sample (dashed line) at F_γ (or θ) larger than the value on the x-axis.

hints at a possible connection between IceCube neutrinos and CRs.

2 STATISTICAL ANALYSIS

Motivated by the hints mentioned above on (1) an HBL origin of some of the IceCube neutrinos from Padovani et al. (2016), and (2) a common origin of neutrinos and CRs from Aartsen et al. (2016b), we have developed a two-step analysis to investigate the connection between γ -ray emitters and CRs.

2.1 Neutrino filter to γ -ray sources ($\nu \rightarrow \gamma$)

The neutrinos are implied here as *filters* in order to single out the best candidate lepto-hadronic accelerators (Petropoulou et al. 2015) from γ -ray catalogs and hence the most probable CR sources. We have used all the high energy catalogs

presently available including the 2FHL, the 2WHSP (Chang et al. 2017), and the 3LAC (Ackermann et al. 2015), as detailed in Padovani et al. (2016) and Tab. 1, focusing on HBL blazars². We have also considered the 2FHL and 3LAC catalogue subsets as reported. The neutrino list is composed of the 51 events (30 starting and 8 tracks) selected by Padovani et al. (2016) and the recently published 29 through going tracks reported in Aartsen et al. (2016a) of which one is a starting track also. No further catalogue has been tested and all the tests performed on the data are reported here not to hide any trial or relevant information.

As done in Padovani et al. (2016), we have filtered γ -ray sources in spatial coincidence with the neutrinos (i.e. within the median angular errors). The selection is done partitioning the flux of the cataloged sources (F_γ) (or alternatively the “figure of merit” (FoM) introduced in the 2WHSP)³. Two subsets of the γ -ray catalogues are then obtained, the neutrino filtered and its complement:

$$(\nu \rightarrow \gamma); F_\gamma \text{ neutrino filter}, \quad (1)$$

$$\setminus(\nu \rightarrow \gamma); F_\gamma \text{ complement}. \quad (2)$$

With respect to Padovani et al. (2016), we have here extended the coverage of the sky for 2FHL to the Galactic plane to allow the realization of neutrino scrambled maps as background cases and included the recently published through going tracks.

2.2 Neutrino filtered sources to CRs ($\nu \rightarrow \gamma \rightarrow \text{CR}$)

In a second independent step, the neutrino selected γ -ray sources at various F_γ (or FoM) are cross correlated with the CRs. The correlation is also done as a function of the angular separation θ between the source and the reconstructed incoming direction of the CRs over the $1^\circ - 30^\circ$ range in steps of 1° . This is because the CRs are charged particles and therefore deflected by an unknown angle due to the intervening magnetic fields.

We quantify the strength of the correlation by counting the number of CR events that have *at least* one neutrino filtered γ -ray source with F_γ at distance smaller than the angular distance θ and compare this to random trials. This is done by randomizing the right ascension of the neutrino events and repeating the statistical analysis mentioned above. This randomization method is regularly used within the IceCube collaboration and ensures that the aforementioned anisotropies in the CRs are conserved and do not artificially contribute to the significance of the result, preserving at the same time the IceCube neutrino distribution, which is known to be not uniformly distributed.

The final probabilities are calculated based on random trials. The final result is corrected for trials due to the scanning in F_γ (or FoM) and θ to search for the largest CR excess

² The determination of ν_S , which is required to classify sources as HBLs, requires the availability of multi-frequency data and is also affected by variability, a defining feature of blazars. The HBL - non-HBL distinction is therefore not sharp by definition.

³ The FoM is defined as the ratio between the synchrotron peak flux of a source and that of the faintest blazar in the WHSP sample already detected in the TeV band.

over the random expectation. We have also corrected for the number of subsets in the 2FHL considering the relative correlations within the subsets. The additional factor is 2.9.

Although the CR horizon is limited by the energy losses caused by the interactions of CRs with photons of the Cosmic Microwave Background (CMB), the so-called GZK (Greisen-Zatsepin-Kuzmin) effect (Greisen 1966; Zatsepin & Kuzmin 1966), we do not apply a-priori cuts on the distance of the cataloged sources. The reason is that a large number of BL Lacs has no measured redshift due to the lack of emission lines in their optical spectra (see also Sec. 4). Moreover, it is difficult to quote a CR horizon a priori. Instead of scanning in redshift z as done in other tests as the one in Aab et al. (2015a) and in Abu-Zayyad et al. (2013a), we use all sources regardless of their redshift.

2.3 Likelihood ratio test

As a last step, a likelihood ratio test comparing the connection between the filtered ($\nu \rightarrow \gamma$) and the complement ($\setminus(\nu \rightarrow \gamma)$) source samples with the CRs is performed. We define the test statistics as

$$\Lambda = \frac{\mathcal{P}((\nu \rightarrow \gamma); F_\gamma \rightarrow CR; \theta)}{\mathcal{P}(\setminus(\nu \rightarrow \gamma); F_\gamma \rightarrow CR; \theta)}, \quad (3)$$

where \mathcal{P} is the probability obtained in the two-step statistical test described above. Large values of Λ indicate preference for a stronger correlation of neutrino filtered γ -ray emitters and CRs supporting a physical connection among the three astronomical messengers. We estimate the significance of this test by comparing data to trials with randomized neutrinos as discussed in the previous section. The p-value is then defined as the chance probability that trials produce a test statistics Λ that is larger than, or equal to that observed.

3 RESULTS

The *neutrino filter* ($\nu \rightarrow \gamma$) introduced in Padovani et al. (2016) selects the γ -ray emitters which are within the median angular errors of the IceCube neutrino events. A significant excess of CRs is here reported in connection with the neutrino filtered 2FHL γ -ray emitters (see Fig. 2 solid lines and Tab. 1). The (F_γ, θ) scan provides as the most significant excess a total of 83 CRs at an angular separation $\theta < 10^\circ$ from the 46 2FHL neutrino filtered γ -ray emitters with $F_\gamma (> 50 \text{ GeV}) \geq 2.5 \times 10^{-11} \text{ ph cm}^{-2} \text{ s}^{-1}$. This number of CRs has to be compared with an expectation of 46.4 random associations determined on neutrino randomized cases. The probability of observing such an excess on randomized maps is 5.5×10^{-5} which translates into 2.2×10^{-3} after compensation for trials.

Among the subsets of γ -ray emitters reported for the 2FHL, the best/minimal probability is obtained for the HBLs + unclassified sample. This sample includes all HBLs plus all sources with $2^\circ < |b_{\text{II}}| < 10^\circ$, which are still unclassified in the catalogue⁴. The scan values where the maximal

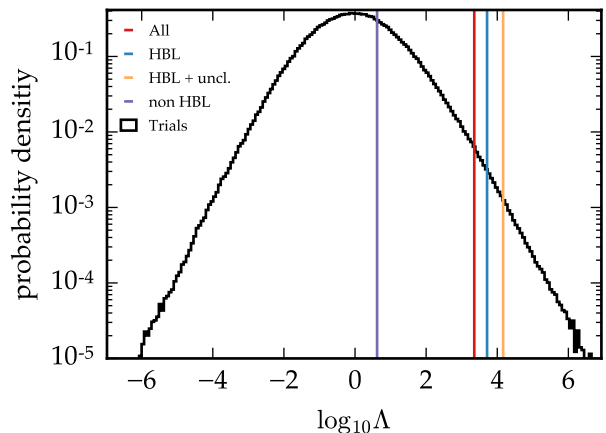


Figure 3. Result of the likelihood ratio test Λ (Eq. 3) for the 2FHL catalogue. Large values of Λ indicate preference of a connection between γ -rays and CRs for the neutrino filtered γ -ray emitters. Vertical lines show the outcome of the statistical test for the subsets of the 2FHL catalogue with respect to random trials (black histogram).

excess is found are $F_\gamma (> 50 \text{ GeV}) \geq 1.8 \times 10^{-11} \text{ ph cm}^{-2} \text{ s}^{-1}$ and $\theta = 10^\circ$. At these scan values, a total of 80 CRs are associated with the neutrino filtered sample, to be compared with an expectation of 42.5 random associations. The probability of observing such an excess on randomized maps is 2.4×10^{-5} which translates into 8.4×10^{-4} (3.14σ) after compensation for trials due to the (F_γ, θ) scan. Moreover, considering the fact that we have tested 4 nested subcatalogues of the 2FHL, the final p-value is 2.4×10^{-3} (2.8σ).

No excess of CRs is found once the complement sample of γ -ray emitters, $\setminus(\nu \rightarrow \gamma)$, is considered (see Fig. 2 dotted lines). A likelihood ratio test Λ (Eq. 3) comparing the connection between the filtered and the complement source samples with the CRs favours a connection between neutrino filtered emitters and CRs (see Fig. 3). With a p-value of 1.8×10^{-4} (2.91σ), the neutrino filter to CRs model is favoured providing a first strong hint of an association between HBLs and CRs. More statistics is required to confirm or disprove this scenario.

For the 3LAC and 2WHSP catalogues, we observe similar but less significant excesses and as for the 2FHL only for HBLs (see Fig. A1, Fig. A2, Fig. A3 and Tab. B1 in the Appendix). Also in these cases, no CR excess is observed for the complement sample of neutrino filtered sources (see dotted lines in Fig. A1, Fig. A2). The result of the likelihood ratio test described above is reported in Fig. A3 and Tab. 1.

sky where the density of stellar sources is still quite high. Despite the fact that the optical counterparts of these γ -ray sources are still unknown, upon inspection, and after the test was carried out, it turned out that most of them have SEDs of the HBL type.

⁴ By excluding the Galactic plane, in fact, there is a high chance that these sources are unrecognized blazars lying in a region of the

Table 1. ($\nu \rightarrow \gamma \rightarrow \text{CR}$) correlation test results: local and global p-values obtained with respect to the γ -ray catalogues tested. The local p-value is the minimum p-value observed partitioning the γ -ray catalogues in F_γ (or FoM) and scanning in angular distance θ between neutrino spatially selected sources and CRs. The global p-value is the corresponding one penalized for the relative trials applied through the two dimensional scan. The p-value calculation is done using $10^6 - 10^7$ trials depending on the significance of the result. The results of the likelihood ratio test in Eq. (3) and the p-value of the outcome are listed in the last two columns.

γ -ray catalogue	#	F_γ (FoM)	$\#(\nu \rightarrow \gamma); F_\gamma$ (FoM)	θ (deg)	#CRs observed	#CRs expected	local p-value ($(\nu \rightarrow \gamma); F_\gamma \rightarrow \text{CR}; \theta$)	global p-value	$\log_{10} \Lambda$	Λ p-value
2FHL	360	0.25	46	10	83	46.4	5.5×10^{-5}	2.2×10^{-3}	3.35	3.1×10^{-3}
HBL	173	0.18	34	10	75	40.6	6.9×10^{-5}	2.0×10^{-3}	3.77	1.6×10^{-3}
+ uncl.	186	0.18	36	10	80	42.5	2.4×10^{-5}	8.4×10^{-4}	4.17	$(6.3 \times 10^{-4})^*$
non-HBL	174	0.35	20	10	37	20.3	1.4×10^{-2}	1.7×10^{-1}	0.62	2.5×10^{-1}
2WHSP	1681	2.51	11	17	75	31.2	3.0×10^{-4}	1.1×10^{-2}	2.57	1.2×10^{-2}
3LAC	1444	0.56	172	18	231	203.4	3.3×10^{-2}	3.3×10^{-1}	0.42	4.2×10^{-1}
HBL	386	0.71	25	16	131	93.4	5.6×10^{-3}	1.1×10^{-1}	1.53	8.2×10^{-2}
FSRQ	415	1.00	50	18	174	166.6	3.6×10^{-1}	9.2×10^{-1}	-1.11	8.6×10^{-1}
other	645	1.00	48	3	19	12.1	4.0×10^{-2}	3.6×10^{-1}	0.08	4.4×10^{-1}

* We apply a further trial factor of 2.9 to account for the 4 nested sub-catalogues.

4 DISCUSSION

Out of the 66 IceCube events, 17 are associated with at least one γ -ray counterpart for our best p-value (2FHL HBLs + unclassified sample). This is one more than in Padovani et al. (2016) because here we do not exclude the Galactic plane; none of these is a track. The fact that no neutrino filtered source appears to be the counterpart of a track-like event is still compatible with the scenario presented here at the 5% level. Hence, if HBLs are neutrinos counterparts they leave room for additional components. All but one of the neutrino filtered γ -ray sources have between one and seven CRs associated within 10° .

As mentioned above, we see 80 CRs for an expectation of 42.5. If these numbers are compared to the total of 303 cosmic rays used in this study, $12.5^{+2.6}_{-2.2}\%$ of the entire CR flux could be interpreted as physically connected to extreme HBLs. This could be an effect of different magnetic field deflections due to different composition population, or additional components in the sources, or a combination of both. We note that this value is intriguingly close to the fraction of the IceCube signal explained by the same type of sources ($\sim 10 - 20\%$) from Padovani et al. (2015) and Padovani et al. (2016).

Among the selected sources, there are also relatively close-by, well-known, TeV emitters such as MKN 421 (also discussed in Fang et al. 2014), PKS 2005-489, and 1ES 1011+496. Given the redshifts of some of the sources (Fig. 4) the scenario proposed here might seem to be in some tension with the expected GZK suppression (and other CR-background interactions). However: 1. the majority of the HBLs do not have a distance determination (and therefore their redshift distribution is not very informative); 2. about half of the sources are expected to be spurious; 3. the intrinsic source power in CRs is unknown.

CRs propagating through space will contribute to the diffuse γ -ray emission via pion photoproduction on the CMB photons. Hence, the scenario proposed here has to be questioned also on these terms. Recent work (Gavish & Eichler 2016) has discussed the contribution of HBLs to the Extragalactic Gamma Ray Background (EGRB) detected by *Fermi*. Given that the EGRB is dominated by HBLs (Giommi & Padovani 2015; Ajello et al. 2015), there is lit-

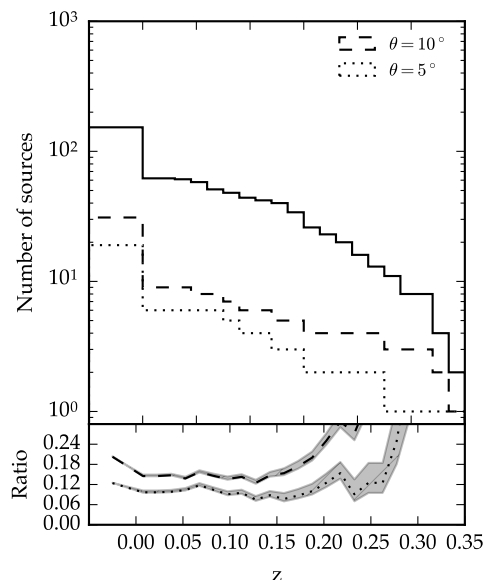


Figure 4. Top: redshift (z) distribution for the 2FHL HBL and unclassified objects (continuous line), at an angular distance $< 10^\circ$ from the CRs (dashed line), and at an angular distance $< 5^\circ$ from the CRs (dotted line). The sources without a measured z are counted in the bin below zero. Bottom: ratio between the two lower lines and the upper line in the top plot.

tle room to accommodate the inevitable diffuse contribution from γ -rays resulting from CR losses during propagation. Once blazar evolution is correctly taken into account as done in Gavish & Eichler (2016), however, the secondary γ -ray radiation expected from HBL blazars, which do not show cosmological evolution and are a small subset of the entire blazar population, is much lower than for other classes leaving these objects as viable sources of CRs. At the same time, the expected cosmogenic (GZK) neutrino flux would also be very low (Taylor et al. 2015).

5 CONCLUSION

We have provided a first hint (p-value = 0.18%; 2.91σ) that a sub-class of blazars may be the counterpart of some high energy neutrinos and CRs. These are extreme blazars, i.e. strong, very high energy γ -ray sources of the high energy peaked type. Due to the limited angular resolution of the IceCube neutrinos and the intrinsic magnetic bending of the CRs, one cannot determine at present which of the counterparts selected is indeed responsible for the multi-messenger emission. Larger samples of CRs, including new data and events with $E < 52 \times 10^{18}$ eV, and of neutrinos, would allow us to test further and with better statistics this first strong hint but unfortunately these data are still proprietary. We therefore suggest the international collaborations to follow up on this or alternatively make their catalogs publicly available as they should be.

ACKNOWLEDGMENTS

We thank the many teams, which have produced the data and catalogues used in this paper for making this work possible. ER is supported by the Heisenberg Program of the Deutsche Forschungsgemeinschaft (DFG RE 2262/4-1, SFB1258), SC by the cluster of excellence ‘‘Origin and Structure of the Universe’’ of the Deutsche Forschungsgemeinschaft.

APPENDIX A: RESULTS FOR THE 2WHSP AND 3LAC CATALOGUES.

Table 1 lists the results for all catalogues used in this work. As highlighted in the discussion section, a strong correlation for HBL type objects in the 2FHL catalogue is found. The 2WHSP catalogue (Chang et al. 2017) consists only of blazars of the HBL type excluding the Galactic Plane ($|b_{\text{II}}| \geq 10^\circ$). The best (lowest) p-value is found for a ‘‘figure of merit’’ $\text{FoM} \geq 2.51$ and CR angular distance $\theta = 17^\circ$. 75 CR events are observed above an expectation of 31.2. The local p-value at this point is 3.0×10^{-4} and increases to 1.1% after trial correction. The scan in FoM and θ is shown in Fig. A1.

The 3LAC catalogue Ackermann et al. (2015) includes HBLs, FSRQ, and other types of sources. As listed in Tab. 1, the most significant result is again obtained for objects of the HBL type, consistent with the result of the 2FHL catalogue. The scan in F_γ and θ is shown in Fig. A2. The most significant correlation is observed for HBL objects with flux $F_\gamma (> 100 \text{ MeV}) \geq 0.71 \times 10^{-8} \text{ ph cm}^{-2} \text{ s}^{-1}$ and $\theta \leq 17^\circ$. 131 CR events are observed above an expectation of 93.4. The local p-value of this observation yields 5.6×10^{-3} . After trial correction this increases to 11%. The other types of objects in the catalogue (FSRQ and others) show a non significant correlation.

The outcome of the likelihood ratio test Λ (Eq. (1)) is shown in Fig. A3 for the 2WHSP (left) and 3LAC catalogue (right). The test for the 2WHSP indicates a result in favour of neutrino filtered sources with a p-value 1.2%. For 3LAC, the result is 8.2%, again more significant for HBLs than for the remaining subsets of the catalog.

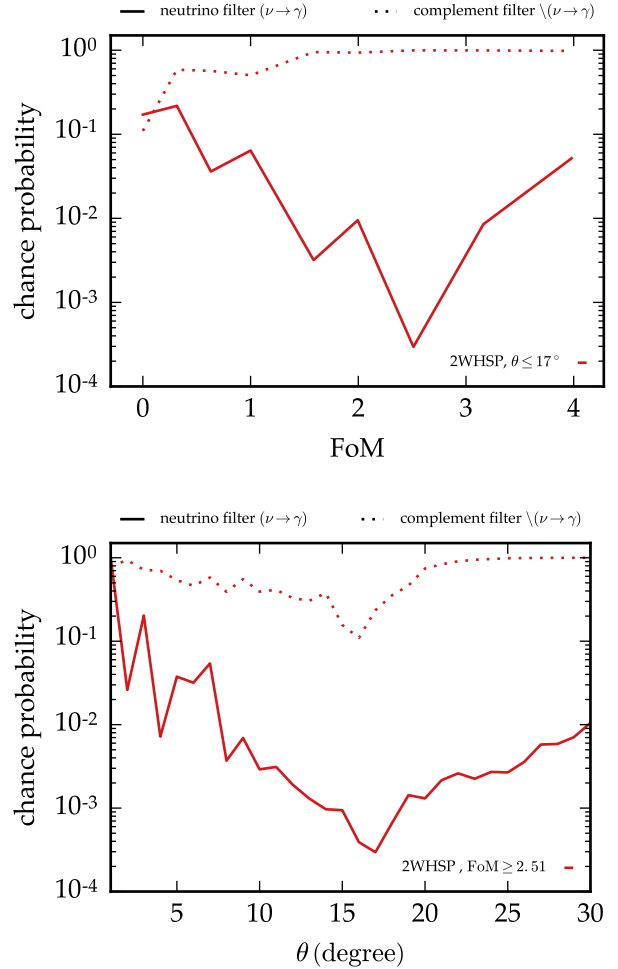


Figure A1. Result of the statistical test for the 2WHSP catalogue scanning over ‘‘figure of merit’’ (FoM, top) and CR angular distance θ (bottom). The probabilities are reported for the neutrino filtered γ -ray emitters (solid line) and for the complement sample (dashed line) at FoM (or θ) larger than the value on the x-axis.

APPENDIX B: CRS IN CORRELATION WITH 2FHL OBJECTS.

The most significant result was seen for neutrinos and CRs correlating with 2FHL objects of the HBL type and unclassified. Tab. B1 lists the clusters of neutrinos correlating with 2FHL objects and CRs. Furthermore, information about the events and objects is listed. Namely: the neutrino energy and angular resolution, the redshift of the object (if known), the position of the CR event, plus its energy and distance from the 2FHL object.

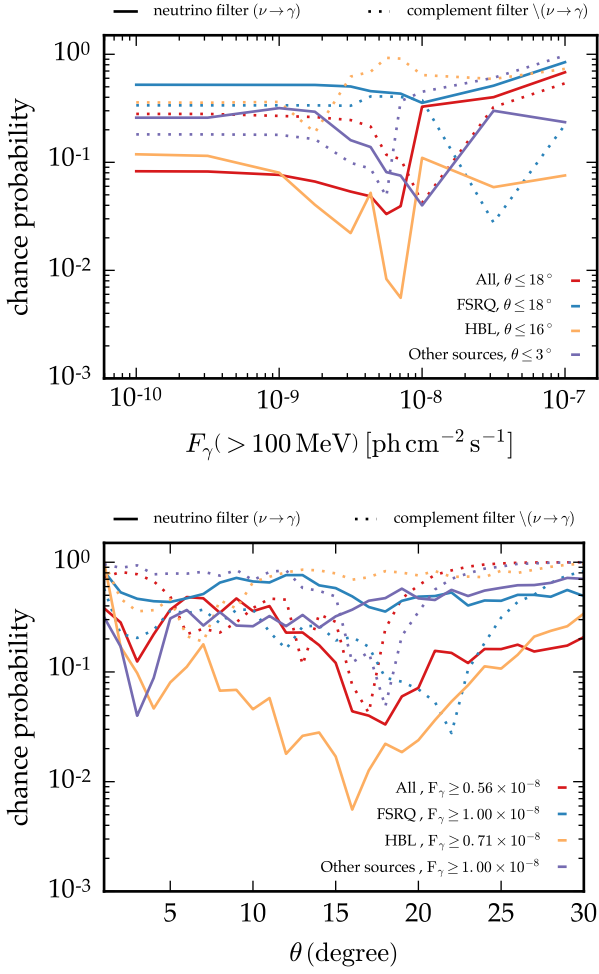


Figure A2. Result of the statistical test for partitions of the 3LAC catalogue over flux $F_\gamma (> 100 \text{ MeV})$ (left) and CR angular distance θ (right). The probabilities are reported for the neutrino filtered γ -ray emitters (solid line) and for the complement sample (dashed line) at F_γ (or θ) larger than the value on the x-axis.

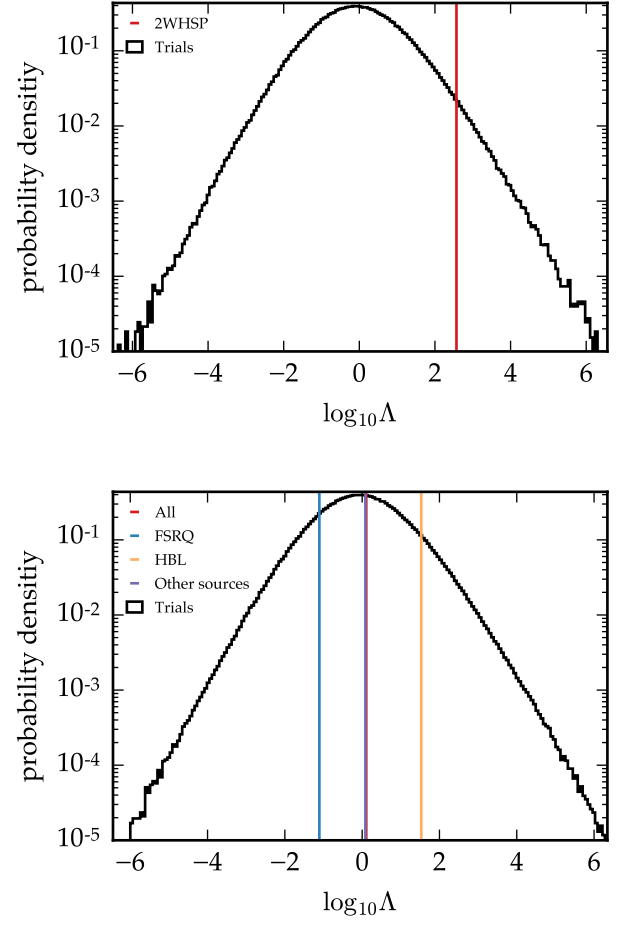


Figure A3. Result of the likelihood ratio test Λ (Eq. 3) for the 2WHSP (left) and partitions of the 3LAC catalogue (right). Vertical lines indicate the outcome of the test using a catalogue with respect to the distribution of random trials (black histogram) as listed in Tab. 1.

Table B1: IceCube neutrinos, 2FHL objects (type HBL and unclassified) and Auger/TA CRs selected in correspondence with the minimum p-value obtained ($F_\gamma (> 50 \text{ GeV}) \geq 1.8 \times 10^{-11} \text{ ph cm}^{-2} \text{ s}^{-1}$ and $\theta \leq 10^\circ$). We report for each neutrino the ID number, the energy and the median angular uncertainty ($\text{median}(\theta)_{\text{IC}}$) as quoted by IceCube; for the γ -ray objects the *Fermi* source name and common name, and if known, the redshift; for the CRs the year of detection, the coordinates, the dataset, the energy and angular distance from the 2FHL object.

High Energy Neutrino			γ -ray Source			Ultra High Energy Cosmic Ray											
ID	Energy (TeV)	$\text{median}(\theta)_{\text{IC}}$ (deg)	2FHL name	Common name	z	Year	RA	Dec	Dataset	Energy (EeV)	θ (deg)						
9	63.2	16.5	J0915.9+2931	B2 0912+29	0.19	2013	138.6	26.1	Auger	62.1	3.4						
						2008	140.0	28.7	TA	59.2	1.0						
						2010	129.0	29.1	TA	60.5	8.5						
			J0910.4+3327	Ton 1015	0.35	2013	138.6	26.1	Auger	62.1	7.4	2008	140.0	28.7	TA	59.2	5.1
												2010	145.0	40.7	TA	92.2	9.1
												2010	137.0	41.5	TA	68.9	8.1
												2010	129.0	29.1	TA	60.5	8.3
												2011	163.7	28.9	TA	62.3	9.5
			J1104.4+3812	MKN 421	0.03	2011	157.0	38.8	TA	72.9	7.3	2012	160.0	35.6	TA	57.4	5.7
												2010	152.4	45.8	TA	79.3	3.7
												2010	139.0	49.6	TA	63.7	9.5
			J1015.0+4926	1ES 1011+496	0.20	2008	152.4	45.8	TA	79.3	3.7	2010	139.0	49.6	TA	63.7	9.5
												2013	165.0	52.4	TA	62.5	7.8
												2013	165.0	52.4	TA	62.5	7.8
			11	88.4	16.7	J1027.0-1749	1RXS J102658.5-174905	0.65	2009	147.2	-18.3	Auger	64.1	9.1			
2011	150.0	-10.3							Auger	100.0	9.9						
2011	149.0	-13.0							Auger	57.2	9.0						
J0952.9-0841	1RXS J095303.4-084003	-				2006	142.3	-13.1	Auger	54.0	7.3	2009	147.0	-18.3	Auger	64.1	9.6
												2011	150.0	-10.3	Auger	100.0	2.4
												2011	149.0	-13.0	Auger	57.2	4.3
												2013	154.0	-15.8	Auger	53.9	9.3
12	104	9.8				J2009.4-4849	PKS 2005-489	0.07	2006	305.6	-46.3	Auger	60.0	3.3			
									2007	315.0	-53.8	Auger	72.7	9.4			
						J1959.6-4725	SUMSS J195945-472519	-	2006	305.6	-46.3	Auger	60.1	4.0	2008	306.0	-55.1
			2008	306.0	-55.1										Auger	55.1	8.7
			2013	308.0	-39.5										Auger	67.3	9.9
			J1936.9-4721	PMN J1936-4719	0.26	2006	305.6	-46.3	Auger	60.1	7.8	2013	287.0	-55.0	Auger	52.9	9.0
												2013	287.0	-55.0	Auger	52.9	9.0
14	1041	13.2	J1713.9-2027	1RXS J171405.2-202747	-	2008	252.7	-22.7	Auger	64.2	5.9						
						2013	284.5	-37.6	Auger	54.4	7.4						
			J1823.6-3454	NVSS J182338-345412	-	2009	286.0	-37.8	Auger	61.0	8.8	2009	276.0	-33.4	Auger	65.8	1.5
												2011	284.0	-28.6	Auger	80.9	9.2
												2011	284.0	-28.6	Auger	80.9	7.1
			J1829.0-2417	1RXS J182853.8-241746	-	2010	284.7	-28.2	Auger	65.2	7.6	2009	276.0	-33.4	Auger	65.8	9.1
												2011	284.0	-28.6	Auger	80.9	7.1
												2010	258.1	-44.9	Auger	72.9	7.0
												2012	260.0	-32.7	Auger	61.8	8.9
												2012	260.0	-32.7	Auger	61.8	8.9
17	200	11.6	J1555.7+1111	PG 1553+113	0.44	2007	245.8	8.5	Auger	54.9	7.3						
						2011	239.0	3.9	Auger	60.3	7.3						
19	71.5	9.7	J0543.9-5533	1RXS J054357.3-553206	0.27	2010	80.2	-64.1	Auger	54.3	9.0						
						2013	92.1	-64.1	Auger	65.4	9.1						
						2013	91.4	-60.6	Auger	72.5	5.8						
20	1141	10.7	J0352.7-6831	PKS 0352-686	0.08	2012	37.0	-75.8	Auger	58.7	9.6						
						2014	45.2	-65.8	Auger	63.6	5.7						
						2010	80.2	-64.1	Auger	54.3	9.8						
						2013	56.6	-67.8	Auger	70.7	0.9						
						2013	64.7	-70.1	Auger	68.8	2.8						
						2014	72.8	-73.5	Auger	60.0	6.8						
22	220	12.1	J1958.3-3011	1RXS J195815.6-30111	0.12	2011	295.1	-27.6	Auger	54.8	4.7						
						2008	304.0	-26.2	Auger	52.6	5.8						
						2011	305.0	-34.5	Auger	67.4	6.6						

Table B1: continued

High Energy Neutrino			γ -ray Source			Ultra High Energy Cosmic Ray								
ID	Energy (TeV)	median(θ) _{IC} (deg)	2FHL name	Common name	z	Year	RA	Dec	Dataset	Energy (EeV)	θ (deg)			
26	210	11.8	J1917.7–1921	1H1914–194	0.14	2010	284.7	-28.2	Auger	65.2	9.8			
						2011	295.0	-27.6	Auger	54.8	9.8			
						2009	294.0	-20.5	Auger	59.5	4.9			
			J1921.9–1607	PMNJ1921–1607	–	2009	294.5	-20.5	Auger	59.5	5.8			
						J0905.7+1359	MG1 J090534+1358	1.07	2011	132.8	12.9	Auger	55.9	3.7
									2007	137.0	6.2	Auger	53.6	7.9
			J0915.9+2931	B2 0912+29	0.19	2009	129.0	15.2	Auger	52.2	6.9			
						2013	138.6	26.1	Auger	62.1	3.4			
						2008	140.0	28.7	TA	59.2	1.0			
						2010	129.0	29.1	TA	60.5	8.5			
27	60.2	6.6	J0816.3–1311	PMN J0816–1311	–	2010	131.9	-15.5	Auger	76.1	7.9			
33	385	13.5	J1933.3+0725	1RXS J193320.3+072616	–	2013	123.0	-6.2	Auger	85.3	7.0			
						2008	287.7	1.5	Auger	118.0	8.2			
						2013	299.0	8.7	Auger	54.6	5.4			
35	2004	15.9	J1931.1+0937	RX J1931.1+0937	–	2011	288.0	0.3	TA	136.0	8.8			
						2008	287.7	1.5	Auger	118.3	9.6			
						2013	299.0	8.7	Auger	54.6	5.9			
			J1942.8+1033	1RXS J194246.3+103339	–	2006	299.0	19.4	Auger	82.0	9.4			
						2013	299.0	8.7	Auger	54.6	3.5			
			J1328.6–4728	1WGA J1328.6–4727	–	2005	199.1	-48.5	Auger	52.1	2.3			
						2006	201.0	-55.3	Auger	69.5	7.8			
						2006	201.0	-45.3	Auger	59.5	2.4			
						2007	200.0	-43.4	Auger	60.0	4.3			
						2008	202.0	-54.9	Auger	53.4	7.4			
J1304.5–4353	1RXS 130421.2–435308	–				2004	199.7	-34.8	Auger	84.7	9.4			
						2005	199.0	-48.5	Auger	52.1	5.1			
						2006	201.0	-45.3	Auger	59.5	3.7			
						2007	200.0	-43.4	Auger	60.0	3.0			
J1307.6–4259	1RXS 130737.8–425940	–				2007	193.0	-35.3	Auger	60.7	9.0			
			2009	194.0	-36.4	Auger	72.5	7.7						
			2004	199.7	-34.8	Auger	84.7	8.4						
			2005	199.0	-48.5	Auger	52.1	5.8						
			2006	201.0	-45.3	Auger	59.5	3.7						
			2007	200.0	-43.4	Auger	60.0	2.4						
			2007	193.0	-35.3	Auger	60.7	8.4						
J1353.5–6640	1RXS J135341.1–664002	–	2009	194.0	-36.4	Auger	72.5	7.0						
			2013	201.0	-34.6	Auger	62.7	9.0						
			2007	195.5	-63.4	Auger	61.9	6.3						
			2008	196.0	-69.7	Auger	71.1	5.5						
			2013	199.0	-63.9	Auger	53.2	4.9						
			2004	208.0	-60.1	Auger	58.6	6.6						
			2008	187.0	-63.5	Auger	65.3	9.3						
			2010	216.0	-66.5	Auger	60.3	3.1						
			2010	219.0	-70.8	Auger	89.1	5.6						
			39	101.3	14.2	J1507.4–6213	–	–	2013	240.3	-68.9	Auger	61.5	8.7
2004	208.0	-60.1							Auger	58.6	9.3			
2007	220.0	-53.9							Auger	61.5	9.2			
J0649.6–3139	1RXSJ064933.8–31391	–				2010	216.0	-66.5	Auger	60.3	6.3			
						2010	219.0	-70.8	Auger	89.1	9.2			
2010	232.0	-56.6				Auger	54.9	6.2						
J0622.4–2604	PMNJ0622–2605	–				2007	105.9	-22.8	Auger	60.8	9.3			
						2007	105.9	-22.8	Auger	60.8	9.9			
						2007	105.9	-22.8	Auger	60.8	7.6			
J0631.0–2406	1RXSJ063059.7–240636	–				–	–	–	–	–	–	–	–	
			J0639.9–1252	–	–	–	–	–	–	–	–			
												J0416.9+0105	1ES 0414+009	0.29
2012	56.4	-3.2	Auger	53.3	9.0									
46	158	7.6	J1027.0–1749	1RXS J102658.5–174905	0.65	2009	147.2	-18.2	Auger	64.1	9.1			
						2011	150.0	-10.3	Auger	100.0	9.9			
						2011	149.0	-13.0	Auger	57.2	9.0			
						2013	154.0	-15.8	Auger	53.9	3.1			
48	104.7	8.1	J1440.7–3847	1RXS J144037.4–38465	–	2004	224.7	-44.0	Auger	58.2	6.2			
						2008	221.0	-42.8	Auger	73.1	4.0			
						2011	219.0	-41.9	Auger	58.8	3.2			

Table B1: continued

High Energy Neutrino			γ -ray Source			Ultra High Energy Cosmic Ray					
ID	Energy (TeV)	median(θ) _{IC} (deg)	2FHL name	Common name	z	Year	RA	Dec	Dataset	Energy (EeV)	θ (deg)
51	66.2	6.5	J0540.5+5822	GB6 J0540+5823	–	2009	99.2	62.7	TA	80.7	8.1
						2010	78.8	61.4	TA	61.2	4.4
						2011	82.5	57.7	TA	74.7	1.6

REFERENCES

- Aab A., et al., 2015a, *Astrophys. J.*, 804, 15
Aab A., et al., 2015b, *Nucl. Instrum. Meth.*, A798, 172
Aartsen M. G., et al., 2013, *Science*, 342, 1242856
Aartsen M. G., et al., 2014, *Phys. Rev. Lett.*, 113, 101101
Aartsen M. G., et al., 2015a, preprint, ([arXiv:1510.05222](https://arxiv.org/abs/1510.05222))
Aartsen M. G., et al., 2015b, *Phys. Rev. Lett.*, 115, 081102
Aartsen M. G., et al., 2016a, *Astrophys. J.*, 833, 3
Aartsen M. G., et al., 2016b, *JCAP*, 1601, 037
Abbasi R. U., et al., 2014, *Astrophys. J.*, 790, L21
Abraham J., et al., 2004, *Nucl. Instrum. Meth.*, A523, 50
Abu-Zayyad T., et al., 2013a, *Astrophys. J.*, 777, 88
Abu-Zayyad T., et al., 2013b, *Nucl. Instrum. Meth.*, A689, 87
Ackermann M., et al., 2015, *Astrophys. J.*, 810, 14
Ackermann M., et al., 2016, *Astrophys. J. Suppl.*, 222, 5
Ajello M., et al., 2015, *Astrophys. J.*, 800, L27
Chang Y.-L., Arsioli B., Giommi P., Padovani P., 2017, *Astron. Astrophys.*, in press
Fang K., Fujii T., Linden T., Olinto A. V., 2014, *Astrophys. J.*, 794, 126
Gaisser T. K., Engel R., Resconi E., 2016, *Cosmic Rays and Particle Physics*. Cambridge University Press
Gavish E., Eichler D., 2016, *Astrophys. J.*, 822, 56
Giommi P., Padovani P., 2015, *Mon. Not. Roy. Astron. Soc.*, 450, 2404
Greisen K., 1966, *Phys. Rev. Lett.*, 16, 748
Halzen F., Zas E., 1997, *Astrophys. J.*, 488, 669
Khiali B., de Gouveia Dal Pino E. M., 2016, *MNRAS*, 455, 838
Kistler M. D., Laha R., 2016, preprint ([arXiv:1605.08781](https://arxiv.org/abs/1605.08781))
Kistler M. D., Stanev T., Yüksel H., 2014, *Phys. Rev.*, D90, 123006
Mannheim K., 1995, *Astropart. Phys.*, 3, 295
Moharana R., Britto R. J. G., Razzaque S., 2016, preprint, ([arXiv:1602.03694](https://arxiv.org/abs/1602.03694))
Muecke A., Protheroe R. J., Engel R., Rachen J. P., Stanev T., 2003, *Astropart. Phys.*, 18, 593
Murase K., Inoue Y., Dermer C. D., 2014, *Phys. Rev.*, D90, 023007
Murase K., Guetta D., Ahlers M., 2016, *Physical Review Letters*, 116, 071101
Neronov A., Semikoz D., 2016, *Phys. Rev. D*, 93, 123002
Padovani P., Giommi P., 1995, *Astrophys. J.*, 444, 567
Padovani P., Petropoulou M., Giommi P., Resconi E., 2015, *Mon. Not. Roy. Astron. Soc.*, 452, 1877
Padovani P., Resconi E., Giommi P., Arsioli B., Chang Y. L., 2016, *Mon. Not. Roy. Astron. Soc.*, 457, 3582
Petropoulou M., Dimitrakoudis S., Padovani P., Mastichiadis A., Resconi E., 2015, *Mon. Not. Roy. Astron. Soc.*, 448, 2412
Schoenen S., Raedel L., 2015, *The Astronomer's Telegram*, 7856
Senno N., Murase K., Mészáros P., 2016, *Phys. Rev. D*, 93, 083003
Tamborra I., Ando S., 2016, *Phys. Rev. D*, 93, 053010
Tavecchio F., Ghisellini G., 2015, *Mon. Not. Roy. Astron. Soc.*, 451, 1502
Taylor A. M., Ahlers M., Hooper D., 2015, *Phys. Rev.*, D92, 063011
Urry C. M., Padovani P., 1995, *Publ. Astron. Soc. Pac.*, 107, 803
Wang X.-Y., Liu R.-Y., 2016, *Phys. Rev. D*, 93, 083005
Zatsepin G. T., Kuzmin V. A., 1966, *JETP Lett.*, 4, 78
Zirakashvili V. N., Ptuskin V. S., 2016, *Astroparticle Physics*, 78, 28

This paper has been typeset from a $\text{\TeX}/\text{\LaTeX}$ file prepared by the author.